JOURNAL OF MATERIALS SCIENCE 26 (1991) 3235–3243

Synthesis and purification of diamond films using the microwave plasma of a CO–H_2 system

YASUSHI MURANAKA, HISAO YAMASHITA, HIROSHI MIYADERA
Hitachi Research Laboratory, Hitachi Ltd., 4026, Kuji-cho, Hitachi-shi, Ibaraki-ken, 319-12 Japan

A variety of diamond films were deposited using the microwave plasma of a CO–H_2 system. Qualities of the synthesized films were correlated with the gas phase atomic hydrogen concentration monitored using optical emission spectroscopy. The amorphous components contained in the synthesized films were of a polyacetylene structure, which was possibly formed by the successive polymerization of C_2H_2 in the gas phase.

Excess atomic hydrogen allowed highly crystallized diamond films to be deposited at high growth rates which included only a small amount of polyacetylene components. Two possible explanations for these results were proposed: the suppression of polyacetylene formation and the production of appropriate precursor (CH_3) for diamond synthesis under the excess atomic hydrogen condition.

Finally, the ratio I_H/I_{Ar} (where I is the optical emission intensity) was suggested as a decisive parameter indicating the suitability of the plasma conditions for the growth of pure diamond with good crystallinity.

1. Introduction

The applications of diamond films have recently been directed towards fabricating diamond transistors and electronic luminescence diodes. There are a number of technical objectives to meet before commercialization of these diamond devices: these include purer diamond growth, defect-free crystal growth, low temperature growth, heteroepitaxy, better surface flatness, and better doping control.

The purpose of this paper is to identify suitable growth conditions for the synthesis of purified diamond films using the microwave plasma of a CO–H_2 system.

Raman analysis is typically employed to determine the degree of diamond crystallinity and the amount of amorphous component in the deposits. The structure of amorphous components are dependent on source gas combinations, such as CH_4–H_2, CH_4–O_2–H_2, CO–H_2 and CH_3OH–H_2, due to the composition change of chemical species in the gas phase. Diamond films synthesized in a CH_4–H_2 system have been well characterized by Raman analysis and usually have broad Raman peaks extending between 1400 and 1600 cm^{-1} [1, 2], other than the diamond peak at 1333 cm^{-1}. They are considered to originate from graphitic carbon or a-C:H (amorphous hydrogenated carbon) formed with diamond. The addition of water or oxygen to the CH_4–H_2 system enhances diamond growth rate, and the deposited films have similar Raman spectra [3, 4] to those prepared in the CH_4–H_2 system [1, 2]. The CO–H_2 system has also been proposed to increase the growth rate of diamond polycrystallites [5].

In a CO–H_2 microwave plasma, glassy carbon was found to grow when a large number of C and C_2 radicals existed in the gas phase. These radicals can be suppressed with hydrogen addition, resulting in the formation of graphite-free diamond films, along with amorphous components showing a broad Raman spectrum between 1400 and 1600 cm^{-1} [6]. The structure of these amorphous components has not been well clarified.

In this paper, the structure of this ambiguous amorphous hydrogenated carbon, codepositing with diamond in a CO–H_2 system, was analysed and suitable diamond growth conditions for suppressing its deposition were determined by investigating the effect of substrate temperature and CO concentration on the properties of the deposited films.

2. Experimental procedure

2.1. Film growth and characterization

The deposition chamber used for diamond growth is described in Fig. 1 along with a plasma emission spectroscopic measurement system which was employed for analysing excited chemical species in the plasma. The chamber dimensions were a 10 mm diameter and a 300 mm length, with a base pressure of 1.3×10^{-2} Pa. A single crystal silicon wafer was used as a substrate, the surface of which was ultrasonically scratched in a methanol–diamond slurry and then cleaned with organic solvents. The substrate was heated in the range of 750 to 850 °C by both microwaves and a nichrome wire heater. The growth temperature was monitored by a thermocouple placed

0022–2461/91 $03.00 + .12 © *1991 Chapman and Hall Ltd.*

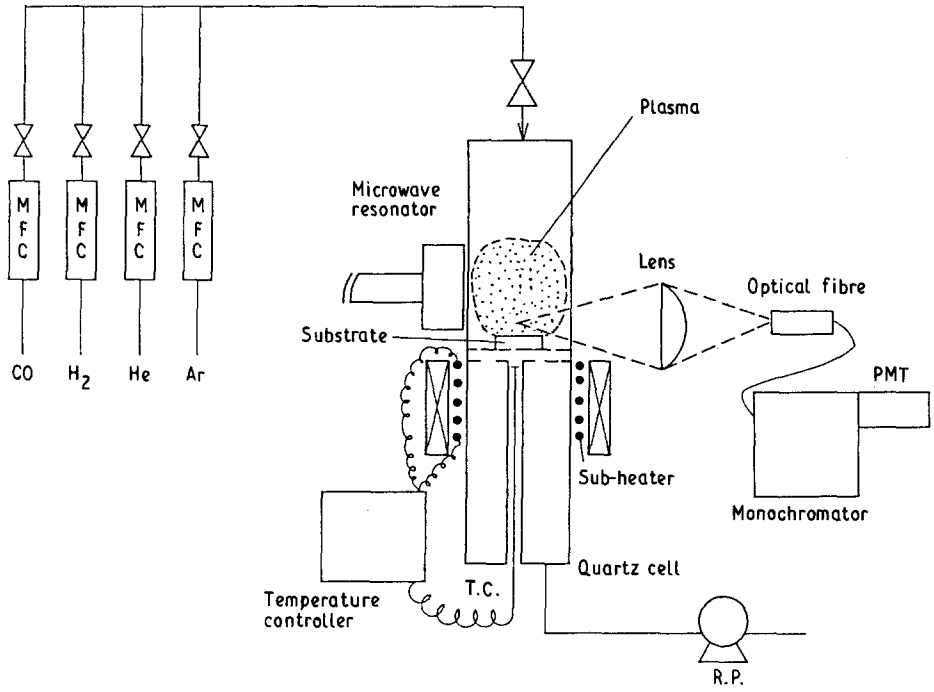

Figure 1 Schematic illustration of experimental apparatus for diamond growth and plasma emission spectroscopy.

below the substrate at a distance of 1 mm. With this arrangement, the thermocouple output could be read without any disturbance of the microwaves.

The microwaves (2.45 GHz, 80 W) were irradiated through a resonator to excite the feed gas. The CO–H_2 system was used in the film growth experiments. The CO concentration (C[CO]) was varied between 1.4 and 14.7% by adjusting both H_2 and CO flow rates at the constant pressure of 248 Pa.

In the optical emission spectroscopic measurements, 5% Ar was added to the CO–H_2 system as a plasma emission actinometer [4, 7].

The crystallinity of the deposits was analysed by both XRD (X-ray diffraction), using the CuK_α line with the incident angle of 1°, and Raman spectroscopy, using an Ar ion laser (514.5 nm) with the output power of 200 mW focused in a diameter of 100 μm. Raman scattering was transferred to a photomultiplier through a slit (1 mm width). The surface morphology and the film thickness were observed by SEM (scanning electron microscopy).

2.2. Optical emission

Optical emissions were transferred from the plasma centre 1 mm above the substrate to a monochromator through an optical fibre after being focused by a quartz lens (focal length = 100 mm) and detected by a photomultiplier. The grating had 1200 lines mm^{-1} grooves and a dispersion of 3 nm/mm. The scanning rate was typically 150 nm min^{-1}.

The plasma emission intensities are dependent on both the concentration of the plasma species in the ground state and the electron energy distribution function of the plasma. The latter also changes with the plasma conditions. It is, thus, difficult to know the relative concentrations of the chemical species of interest using the emission intensities, particularly when the plasma parameters are changed.

A recent theoretical treatment [7] has proposed plasma emission actinometry which is capable of correlating the emission intensities with the relative concentrations of the plasma species using an inert reference gas. The relative concentration of fluorine atom in the ground state was determined using Ar as an actinometer [7].

The same technique has been recently employed to compare the relative atomic hydrogen concentration (C[H]) in a diamond deposition system (CH_4–O_2–H_2) [4].

In the present experiments, 5% Ar was added to a CO–H_2 mixture and the intensity ratio of the hydrogen Balmer line (656.3 nm) to the Ar line (750.4 nm) was monitored as relative C[H] under different plasma conditions.

3. Results

The details of growth conditions and the results of characterization of obtained films are described in Table I (noted as films A–G). The SEM images of these films are depicted in Fig. 2.

3.1. Effect of substrate temperature on film properties

Diamond films grown at the substrate temperatures of 750, 800, and 850 °C are marked as A, B, and C, respectively. C[CO] was 1.4% at constant flow rates of CO and H_2.

Almost the same film growth rates were obtained as shown in Table I, which suggests that the film growth reaction is diffusion-controlled in this temperature region. According to the SEM images in Fig. 2, the (111) plane is dominant on the surface of all the samples a to c, which is consistent with an earlier finding [8] indicating that the (111) plane was preferably grown at a low methane concentration of 0.4% in

TABLE I Experimental conditions and the results of film characterization

Notation	Flow rate (sc cm)		C[CO] (mol %)	Substrate temperature (°C)	Growth rate (μm h^{-1})	XRD INT. Ratio[a]			W_{int}[b] (DEG)	I_a/I_D[c]	I_H/I_{Ar}[d]
	CO	H_2				(111)	(220)	(311)			
A	3	206	1.4	750	0.25	100	20	11	0.50	19.8	2.42
B	3	206	1.4	800	0.25	100	20	8	0.57	—	2.36
C	3	206	1.4	850	0.23	100	25	12	0.53	11.9	2.40
D	5.4	209	2.5	750	0.27	100	20	9	0.62	37.3	2.60
E	41.6	242	14.7	750	0.77	100	24	13	0.70	19.3	1.47
F	5.4	108	4.8	750	0.78	100	21	10	0.45	—	3.92
G	5.4	73	6.9	750	1.18	100	66	14	0.46	6.3	4.96

[a] X-ray diffraction intensity ratio.
[b] Integrated width.
[c] I_a/I_D Raman scattering intensity ratio of I_a (1450 cm^{-1}) against I_D (1333 cm^{-1}).
[d] I_H/I_{Ar} Optical emission intensity ratio of H_α (656.3 nm) against Ar (750.4 nm).
Total Pressure 248 Pa.

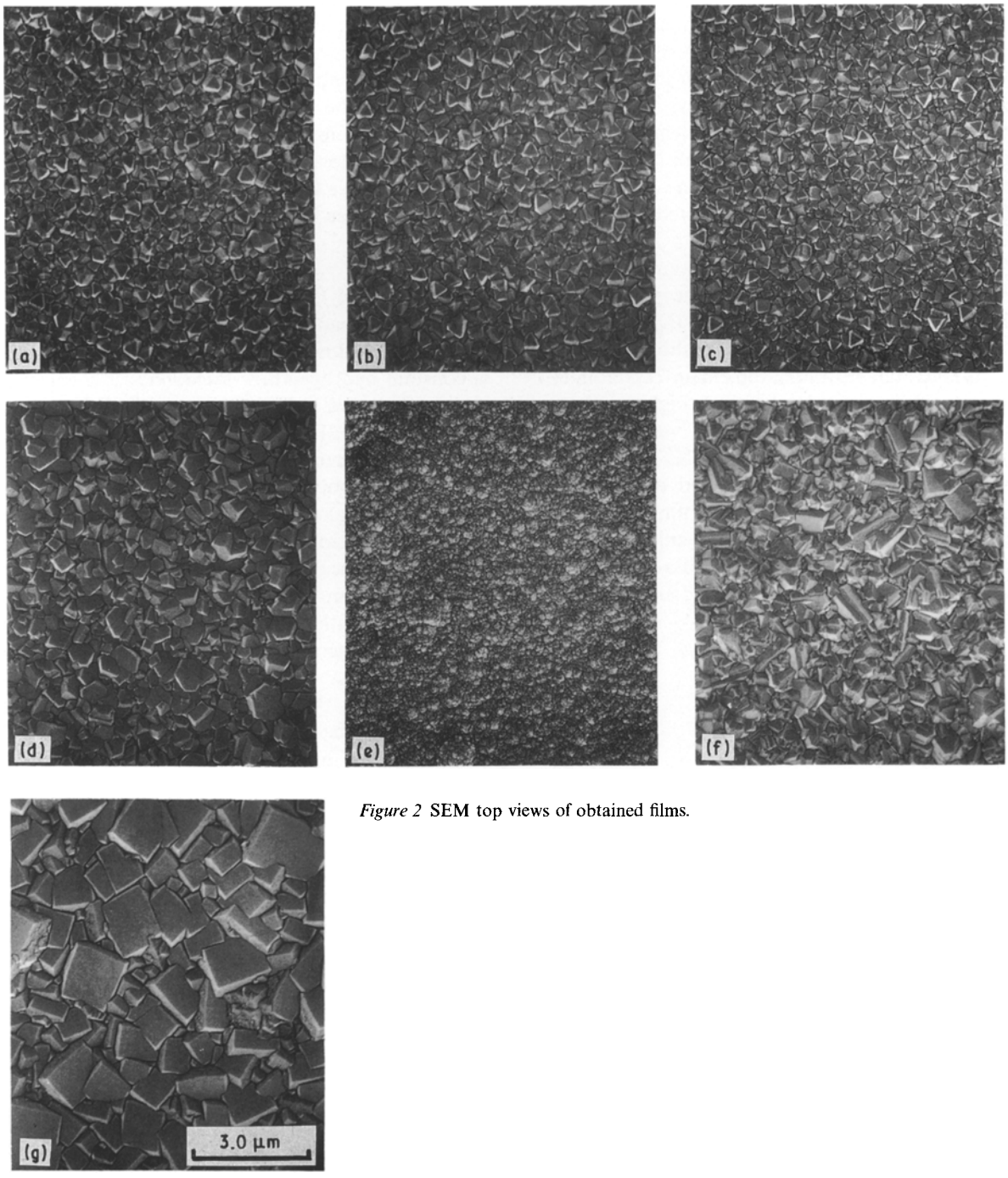

Figure 2 SEM top views of obtained films.

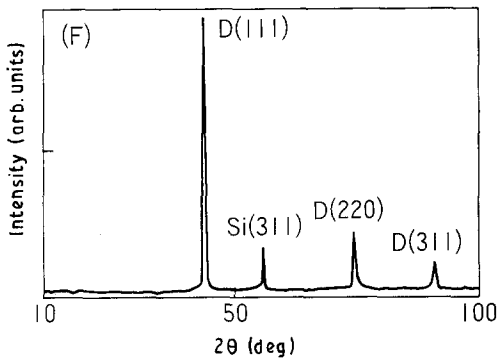

Figure 3 Typical X-ray CuK_α diffraction patterns. (D diamond, Si silicon)

the CH_4–H_2 system. The same phenomenon was also observed in the CO–H_2 system (C[CO] = 1.4%).

Typical XRD patterns are shown in Fig. 3. Three peaks associated with the diamond (111), (220), and (311) planes were observed, the intensity ratios of which are shown in Table I.

W_{int} (integrated width also shown in Table I) was used to compare the degree of crystallinity of the deposits, which was calculated by dividing the integrated area of the strongest (111) peak in Fig. 3 by its maximum height for normalization. The diamond film with a narrow W_{int} is considered to be highly crystallized.

Almost the same XRD patterns were obtained for films A, B, and C according to the peak intensity ratios, and no clear dependence of W_{int} on the substrate temperature was observed, as shown in Table I. This implies that no improvement in crystallinity of the diamond films occurred even in high temperature growth.

Raman spectra for films A and C are shown in Fig. 4. Both had a barely observed diamond peak at 1333 cm^{-1}, and a broad spectrum with a peak near 1450 cm^{-1}. Diamond films synthesized in the CH_4–H_2 microwave plasma [2] had a similar broad Raman spectrum with a peak near 1500 cm^{-1} which

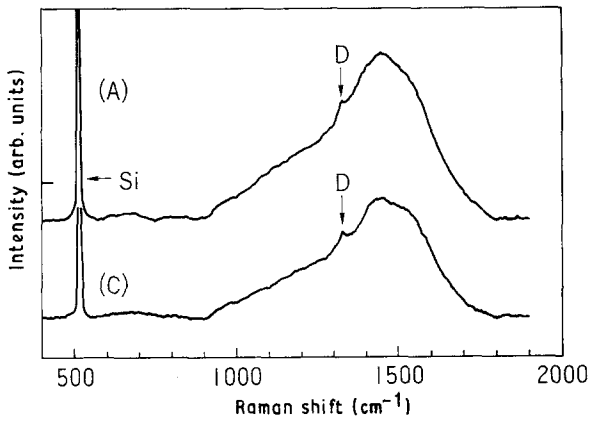

Figure 4 The Raman spectra of diamond films synthesized at different substrate temperatures. (A 750 °C, C 850 °C) (Feed gas CO(1.4%)–H_2(BAL.), total flow rate 209 sccm, total pressure 248 Pa, growth time 3 h, D diamond (1333 cm^{-1}), Si silicon (520 cm^{-1}).)

was suggested to originate from amorphous components.

Another study of diamond films grown in the CH_4–H_2–O_2 system [4] showed a broad spectrum with a peak near 1530 cm^{-1} which was also considered to originate from graphitic or amorphous carbon. The structure of films A and C are thus different from the films mentioned above based on deviation in the Raman shift frequency, and possibly inherent in the CO–H_2 system. Details leading to the conclusion are explained later.

I_a/I_D (shown in Table I) was defined to compare the amount of amorphous components in diamond films. I_a and I_D are the Raman scattering intensities at 1450 and 1333 cm^{-1}, respectively, the former corresponds to amorphous components and the latter is associated with diamond.

According to I_a/I_D values in Table I, there was a small drop in the amount of amorphous components on increasing the substrate temperature from 750 to 850 °C (films A and C), however complete removal of the amorphous component was difficult by simply raising the substrate temperature above 750 °C because of the appearance of a broad Raman spectrum even for film C synthesized at 850 °C. This implied that the amorphous networks were thermally stable and their formation may relate instead to the chemical species in the gas phase.

3.2. Effect of CO flow rate

C[CO] was changed in the range of 1.4 to 14.7% by varying CO flow rate (3 to 41.6 sccm) at almost a constant hydrogen flow rate (206 to 242 sccm). The films A, D, and E were deposited at the CO concentrations of 1.4, 2.5, 14.7%, respectively. According to the XRD peak intensity ratios in Table I, these films consisted of polycrystallites with almost the same diamond crystal orientation as films B and C.

Raman spectra indicated clear differences in Fig. 5. The diamond peak at 1333 cm^{-1} of film D was smaller than that of film A in intensity, which meant that the amount of synthesized diamond became less when C[CO] was increased to 2.5% (film D) from 1.4% (film A).

Interestingly, the Raman spectrum was completely changed with the further increase of C[CO] to 14.7% (film E). Film E had a number of sharp peaks at 1550, 1465, 1355 and 1130 cm^{-1} in addition to the diamond peak at 1333 cm^{-1}. A polyacetylene crystalline film was also analysed as a reference. It was deposited on a silicon substrate by plasma assisted polymerization and its Raman spectrum is also depicted in Fig. 5.

The polyacetylene reference film had peaks at 1550, 1355, 1460–1500, 1140–1185 cm^{-1}. The former two peaks corresponded to cis-$(CH)_x$ [9] and the latter two peaks were associated with trans-$(CH)_x$ [10–12]. Each peak of film E was observed at almost the same Raman shift as the polyacetylene reference, and gave a quite similar pattern. Film E thus turned out to have a network of diamond polycrystallites and amorphous hydrogenated carbon in a partly crystallized polyacetylene structure. The surface morphology of film E

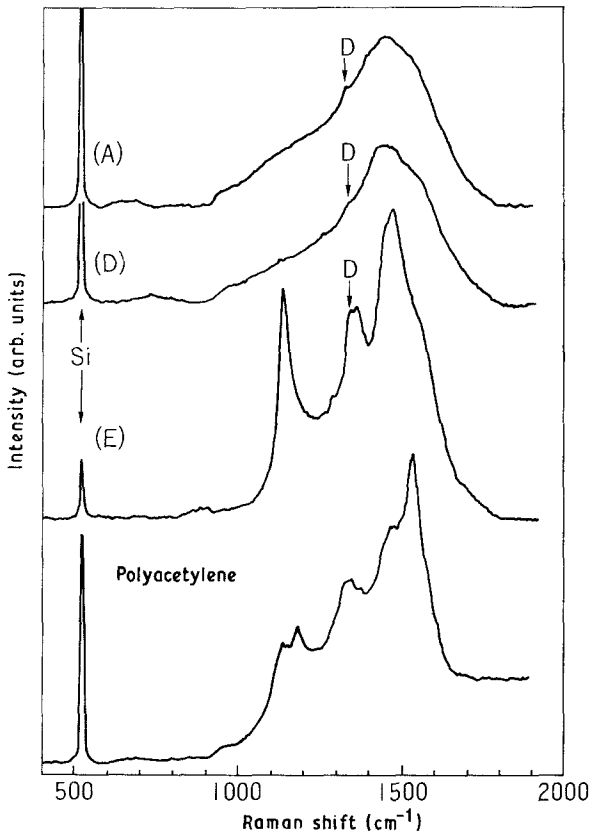

Figure 5 The effect of CO flow rate in sc cm on the Raman spectra of synthesized films. (A 3/206, D 5.4/209, E 41.6/242) (CO concentration (A) 1.4%, (D) 2.5%, (E) 14.7%, total gas pressure 248 Pa, growth time 3 h, substrate temperature 750 °C, D diamond (1333 cm^{-1}), Si silicon (520 cm^{-1}).)

(Fig. 2) was totally different from the other films, and showed no well-defined crystal facets, rather it had a microcrystalline phase.

Raman spectra of films A and D had a broad shoulder near 1550 cm^{-1} and broad peaks near 1450 cm^{-1}. Additionally, film D had a small peak at 1130 cm^{-1}. These peaks were the same as those of film E in position, but they were broader. Considering the fact that a Raman peak usually widens with deterioration in crystallinity, the peak broadening for films A and D was thought to represent an amorphous polyacetylene structure.

Comparing W_{int} and I_a/I_D between films A, D, and E (Table I), highly crystallized diamond films (narrow W_{int}) with less polyacetylene components (small I_a/I_D) were obtained at a lower flow rate of CO (at lower C[CO]).

3.3. Effect of hydrogen flow rate

C[CO] was varied by changing the hydrogen flow rate with a constant CO flow rate of 5.4 sc cm. Films D, F, and G were deposited at CO concentrations of 2.5, 4.8, and 6.9%, respectively.

Highly crystallized films were first expected at a lower CO concentration as is the case in Section 3.2, but, to the contrary, films with better crystallinity (narrow INT. W), with less polyacetylene components (small I_a/I_D), were obtained at higher C[CO] (lower hydrogen flow rate) for films D, F, and G (Table I). Additionally, larger growth rates were obtained at higher C[CO] (Table I).

The Raman spectra of films D and G are shown in Fig. 6. Among all the samples, the sharpest diamond peak was observed for film G.

It was previously reported [8] that the (100) plane was preferably grown at a high CH_4 concentration in the CH_4–H_2 system. In the CO–H_2 system, both (111) and (220) planes became dominant on increasing C[CO] (see the intensity ratios of film G in Table I).

What became clear from the results of Sections 3.2 and 3.3 was that CO concentration was not a decisive factor for either crystallinity or polyacetylene inclusion. It was difficult to correlate the film properties represented by W_{int} and I_a/I_D with the growth conditions, such as flow rates and mole fractions. The drastic change in film properties observed was considered to be due to the composition change of the chemical species in the plasma. This recalled previous mass spectroscopic studies of CO–H_2 glow discharge [13], which confirmed the existence of various hydrocarbons and oxygen-involving species like CH_x and H_xCO (x = 1 to 4), and a number of etchants of non-diamond components, such as OH, O, O_2, and H. These species were also considered to be produced in the present system and to have significant influence on the film properties. In particular, atomic hydrogen was focused on among these important species. The atomic hydrogen is known to prevent C and C_2 radicals from being produced both in the gas phase and on a growing surface [6], so it was considered to have a possibility for eliminating amorphous hydrogenated carbon. Another reason for focusing on the atomic hydrogen was that the relative atomic hydrogen density can be easily obtained, even under different plasma conditions by an advanced monitoring technique called plasma emission actinometry [4, 7]. On the other hand, advanced optical absorption methods are required to detect other species like

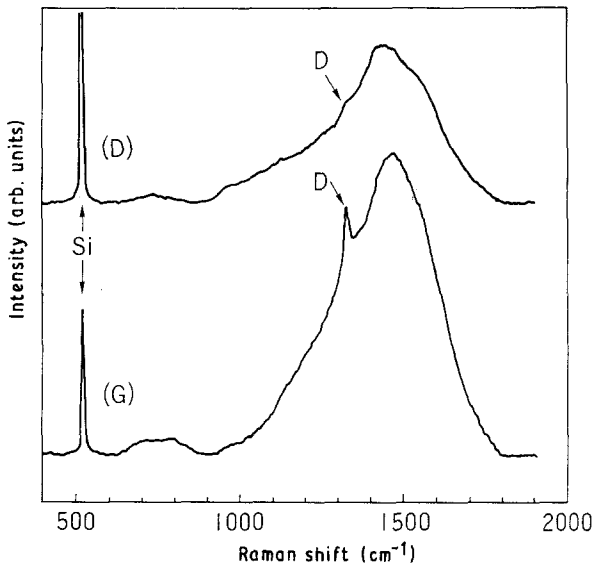

Figure 6 The effect of hydrogen flow rate on the Raman spectra of synthesized films. (D 5.4/209, G 5.4/73) (CO concentration (D) 2.5%, (G) 4.8%, total pressure 248 Pa, growth time 3 h, substrate temperature 750 °C, D diamond (1333 cm^{-1}), Si silicon (520 cm^{-1}).)

TABLE II The observed electronic transition in a CO–H_2 plasma

Chemical species	Electronic transition	Band system	Intensity
CO	$b^3\Sigma$–$a^3\Pi$	The third positive and 5B	L
CO	$B^1\Sigma$–$A^1\Pi$	The angstrom	M
OH	$A^2\Sigma^+$–$X^2\Pi$	306.4 nm	M
CH	$A^2\Delta$–$X^2\Pi$	430.0 nm	S
H_α	2P–3D	—	L
H_β	2P–4D	—	L
H_γ	2P–5D	—	S
C_2	$C^1\Pi g$–$b^1\Pi u^+$	Deslandres–D'azambuja	VS
C_2	$A^3\Pi g$–$X'^3\Pi u$	Swan	VS

CH_x(x = 2 to 4) and H_xCO(x = 1 to 4), which are extremely difficult to monitor. The relative atomic hydrogen concentration was measured for a possible correlation of C[H] with diamond film properties.

3.4. Emission lines

Typically observed emission lines are listed in Table II. Atomic carbon was not detected. The silicon line (288.2 nm) was not observed under the plasma conditions shown in Table I, implying that the quartz etching was fully suppressed.

3.5. Relative atomic hydrogen concentration

In order to clarify the role of gaseous atomic hydrogen during diamond film growth, C[H] should be monitored under the same conditions as in the film growth. The relative intensity of H_α (656.3 nm) against Ar (750.4 nm) (noted as I_H/I_{Ar}) was actually monitored because it is proportional to C[H] [4]. The effects of substrate temperature, the CO flow rate, and the hydrogen flow rate were investigated.

Substrate temperature dependence is shown in Fig. 7. There was an increase of I_H/I_{Ar} with the temperature drop. This was in good agreement with the comments in a previous study [4] that C[H] increased with a wall temperature drop due to fewer recombinations of atomic hydrogen occurring on the wall at low temperature.

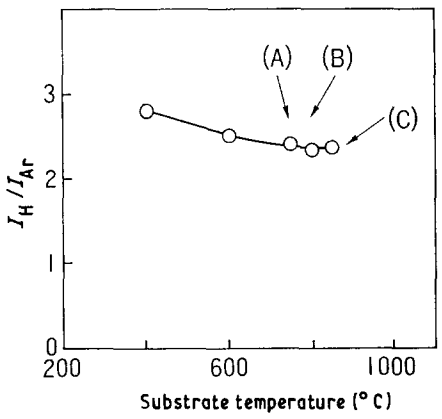

Figure 7 The effect of substrate temperature on the atomic hydrogen concentration in CO–H_2–Ar plasma. (Feed gas CO(1.4%)–Ar(5%)–H_2(BAL.), total flow rate 220 sccm, total pressure 248 Pa.)

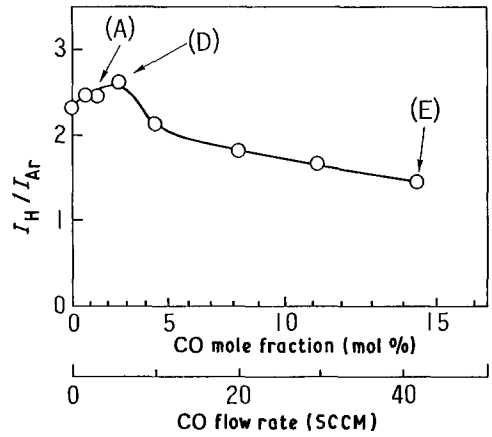

Figure 8 The relative concentration of atomic hydrogen as a function of CO flow rate. (Ar density 5 mol %, hydrogen flow rate 203 to 245 sccm, total pressure 248 Pa, temperature 750 °C)

Wall temperature (T_w) dependence on substrate temperature (T_s) was observed using a pyrometer. T_w turned out to change between 370 and 730 °C when T_s was adjusted between 400 and 750 °C, thus, the increase of I_H/I_{Ar} with lowering of T_s may relate to the change of T_w as suggested earlier [4].

The growth conditions for films A to C are indicated in Fig. 7. In the temperature region (750 to 850 °C) where these films were grown, almost the same amount of atomic hydrogen existed in the gas phase.

CO flow rate dependence is shown in Fig. 8. I_H/I_{Ar} increased with small addition of CO to pure hydrogen, and then gradually decreased with the further addition of CO.

Dicarbon was observed depending on the gas mixing ratio, which implies the existence of oxygen in the plasma. Oxygen has the effect of suppressing the wall recombinations of atomic hydrogen [14]. Thus, the slight increase of I_H/I_{Ar} in Fig. 8 may be due to the small amount of oxygen produced through the direct decomposition of CO. The growth conditions for films A, D, and E are indicated in Fig. 8.

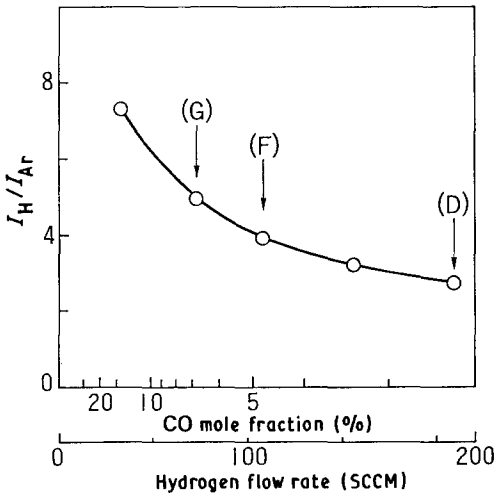

Figure 9 The relative concentration of atomic hydrogen as a function of hydrogen flow rate. (CO flow rate, 5.4 sccm, Ar density 5 mol %, total pressure 248 Pa, temperature 750 °C)

Fig. 9 shows the dependence of molecular hydrogen flow rate on I_H/I_{Ar} at a constant CO flow rate. I_H/I_{Ar} decreased on increasing molecular hydrogen flow rate, which meant that a large amount of atomic hydrogen was produced when the mole fraction of molecular hydrogen was small. The growth conditions for films D, F, and G are indicated in Fig. 9.

3.6. Relationship between I_H/I_{Ar}, W_{int}, and I_a/I_D

W_{int} and I_a/I_D of synthesized films A to G are plotted in Fig. 10 against I_H/I_{Ar} (shown in Figs 7 to 9 and Table I) monitored near the substrate under the actual growth conditions. The growth rates are also shown together in Fig. 10.

Interestingly, both W_{int} and I_a/I_D turned out to decrease on increasing I_H/I_{Ar}, indicating that the deposited films were more highly crystallized, and polyacetylene formation was suppressed on increasing the amount of atomic hydrogen in the gas phase. This implied that I_H/I_{Ar} was an important parameter which allowed the appropriate plasma conditions to be determined for the synthesis of purified diamond with good crystallinity in the CO–H_2 system.

The growth rate had a minimum at the critical value of $I_H/I_{Ar} = 2.4$. Beyond this point, the deposits (A to D, F, and G) had similar crystal phases as shown in Fig. 2, and the growth rates became larger on increasing I_H/I_{Ar}.

Film E grown at a smaller value of I_H/I_{Ar} than 2.4 had a totally different crystal phase as shown in Fig. 2, and the Raman spectrum inherent to polyacetylene as shown in Fig. 5, thus, polyacetylene formation and a microcrystalline phase may contribute to a relatively large growth rate of film E as shown in Fig. 10.

From investigating the relationship of the film properties and I_H/I_{Ar}, it was seen that highly purified diamond films with good crystallinity could be produced under an excess atomic hydrogen condition.

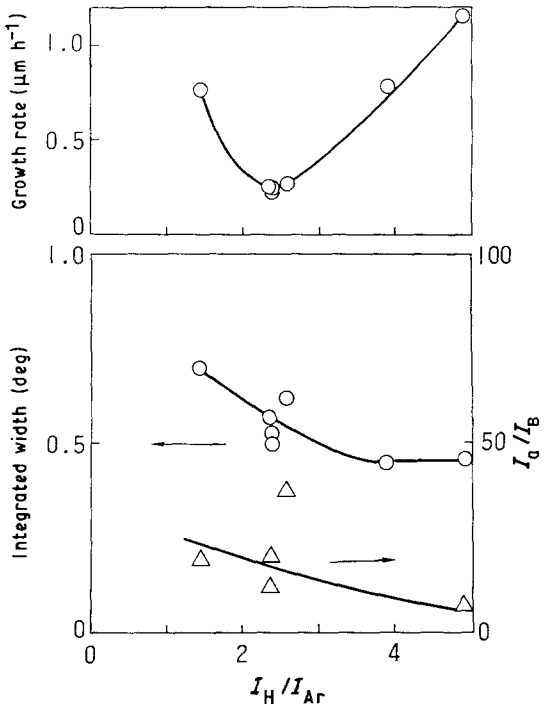

Figure 10 The effect of relative concentration of atomic hydrogen on the growth rate and the crystallinity of the deposits. (I_a/I_D Raman scattering intensity ratio of I_a (1450 cm^{-1}) against I_D (1333 cm^{-1})

4. Discussion

Although very weak emission of dicarbon was observed in the optical emission studies, no trace of graphite formation in the CO–H_2 microwave plasma system was detected by film characterization.

A previous paper [5] found that graphite could be synthesized in a CO microwave plasma. This graphite had twin broad peaks at 1360 and 1560 cm^{-1} (by Raman analysis) inherent to so-called glassy carbon consisting of graphite microcrystallites. The diamond films synthesized in the present experiments had no such peaks in the Raman spectra as shown in Figs 4 to 6.

Gas phase emission studies of a CO–He–H_2 system [6] found that a large amount of carbon and dicarbon radicals were produced in a CO–He microwave plasma when graphitic carbon was formed on the substrate. In the present growth experiments, only very weak emission of dicarbon was observed, which indicated that there was little possibility that the films grown involved graphite or graphitic carbon. The amorphous components contained in films A to G thus primarily consisted of a polyacetylene structure.

When the plasma emissions had a larger value of I_H/I_{Ar}, more highly crystallized diamond films with less polyacetylene components could be produced at a higher growth rate (Fig. 10). Two reasons could be considered to explain these results, such as the suppression of polyacetylene formation and the production of appropriate precursors for diamond crystallites.

Polyacetylene formation in a CO–H_2 system can be explained by the following mechanisms. Unsaturated carbon atoms may exist on the surface under a deficiency of atomic hydrogen and be attacked by a number of precursors in the gas phase. Mass spectroscopic studies of a CO–H_2 glow discharge [13] detected unsaturated hydrocarbons like C_2H_2 in addition to saturated hydrocarbons such as $CH_x (x = 1$ to 4), C_2H_6 and C_6H_8, in the gas phase. When unsaturated hydrocarbon like C_2H_2 in the gas phase attack the unsaturated surface carbons $(\equiv C\cdot)_s$, polyene chains are considered to be successively formed through the following reactions

$$(\equiv C\cdot)_s \overset{C_2H_2}{\Leftrightarrow} \equiv C\text{–}CH{=}CH\cdot$$

$$\overset{C_2H_2}{\Leftrightarrow} \equiv C\text{–}CH{=}CH\text{–}CH{=}CH\cdot \quad (1)$$

Under an excess atomic hydrogen environment (I_H/I_{Ar} is large), unsaturated carbons on a growing surface will be stabilized by attaching atomic hydrogen to make sp^3 C–H bonds, as suggested by previous work [15, 16].

$$(\equiv C\cdot)_s \overset{H}{\Rightarrow} (\equiv CH)_s \quad (2)$$

The surface density of the unsaturated carbon atoms will drop on increasing C[H]. Under this condition, the forward reaction of Equation 1 is suppressed because of the disappearance of unsaturated carbons $(\equiv C\cdot)_s$.

On the other hand, polyene chain formation are suppressed by combining their dangling bonds with excess atomic hydrogen as seen in the next equation

$$\equiv C\text{–}CH{=}CH\text{–}CH{=}CH\cdot \overset{H}{\Rightarrow} (\equiv C\text{–}CH{=}CH\text{–}CH{=}CH_2) \quad (3)$$

The polyacetylene formation was thus considered to be suppressed on increasing I_H/I_{Ar}, as shown in Fig. 10. This causes the selective growth of diamond at the growing sites (denoted by [d–S]) by the attack of diamond precursors in the gas phase (denoted by [d-precursor]$_g$) in the following

$$[\text{d–S}] + (\text{d-precursor})\text{g} \Rightarrow \text{Diamond} \quad (4)$$

In an excess atomic hydrogen environment, diamond is preferably grown because diamond growing sites can be protected from being blocked by polyacetylene formation through bond stabilization with atomic hydrogen in Equation 2. A typical case is film G synthesized with a large amount of atomic hydrogen in the gas phase ($I_H/I_{Ar} = 4.96$), as shown in Fig. 9. Film G consisted of highly crystallized diamond ($W_{int} = 0.46°$) with clear crystal facets in large sizes (shown in Fig. 2) and a small number of polyacetylene components ($I_a/I_D = 6.3$).

On the other hand, film E was deposited with a shortage of atomic hydrogen where diamond growing sites are thought to be blocked due to the interference of gas-phase polyacetylene precursor (noted as [PA-precursor]g) by the following

$$[\text{d–S}] + [\text{PA-precursor}]\text{g} \Rightarrow \text{Polyacetylene chain} \quad (5)$$

Film E was thus considered to show the deterioration of the crystallinity ($W_{int} = 0.7°$) caused by a large amount of polyacetylene inclusion ($I_a/I_D = 19.3$), resulting in the appearance of a microcrystalline phase (Fig. 2).

Considering that the XRD peak width is usually broadened with crystal size reduction, another reason for the widening of W_{int} of film E may be due to the microcrystalline phase as a result of much polyacetylene inclusion. These considerations led to a conclusion that excess atomic hydrogen allowed highly purified diamond films with good crystallinity to be deposited at high growth rates, as shown in Fig. 10.

The observed drastic changes of diamond film properties could also be explained by the composition changes of hydrocarbons in the gas phase.

The production of CH_3 and C_2H_2 was focused on referring to mass spectroscopic studies of CO–H_2 glow discharge [13] because it has been suggested that these species are important precursors for diamond synthesis [17–20]. The amounts of CH_3 and C_2H_2 were the same order of magnitude when C[CO] was higher than 10%, and the fraction of C_2H_2 increased with C[CO] [13]. The mole fraction ratio of CH_3 to C_2H_2 (noted as $C[CH_3]/[C_2H_2]$) was, however, significantly large when C[CO] was near 10%, and presumed to approach a constant large value when C[CO] was smaller than 10% [13].

Fig. 8 shows the relative atomic hydrogen concentration as a function of CO mole fraction, at which films A, D, and E were synthesized. Comparing the properties of these films in Table I, more highly crystallized diamond films with less polyacetylene components turned out to be obtained at lower C[CO], as seen before.

As shown in Fig. 8, film E consisting of a large amount of polyacetylene component was synthesized at the CO mole fraction of about 14.7% where a large amount of C_2H_2 was considered to exist in addition to CH_3 [13]. C_2H_2 is thus thought to relate to polyacetylene formation as indicated in Equation 1. Films (A) and (D) having clear crystal facets were grown at lower CO concentration than 10% where a larger amount of CH_3 was thought to be produced than that of C_2H_2 [13], which supports the previous work suggesting the importance of CH_3 as a precursor for diamond [17–19]. These considerations led to the conclusion that CH_3 is an important precursor for diamond and C_2H_2 is a precursor for polyacetylene chains, and the gas phase composition with a large fraction ratio of CH_3 to C_2H_2 ($C[CH_3]/C[C_2H_2]$) is appropriate for growth of purified diamond films with good crystallinity. Interestingly, plasma emissions showed a higher value of C[H] when the ratio $C[CH_3]/C[C_2H_2]$ was considered to increase, in reference to [13] and Fig. 8. This implies that I_H/I_{Ar} can be a decisive parameter showing the suitability of the composition of plasma species for diamond growth.

As indicated in Table I and Fig. 9, purified diamond films with good crystallinity were obtained at high C[CO] when CO flow rates were constant and molecular hydrogen flow rates were changed. All films of D, F, and G were synthesized at lower CO mole fractions than 10%, where $C[CH_3]/C[C_2H_2]$ was considered to be large and constant, as mentioned before. This is the reason that the above films were well crystallized as shown in Fig. 2. More highly crystallized films with less polyacetylene components were, however, obtained at higher growth rates on increasing C[CO] as is the case of films D, F, and G indicated in Table I. This is considered to relate to the increase of atomic hydrogen concentration on increasing C[CO] as shown in Fig. 9. Atomic hydrogen had the effect of suppressing polyacetylene formation by stabilizing dangling bonds of both unsaturated carbons and polyacetylene chains as indicated in Equations 2 and 3. This was considered to enhance the selective growth of diamond (Equation 4), resulting in the production of purified polycrystallites at a large growth rate.

In the CO–H_2 system, the large value of I_H/I_{Ar} indicated that the plasma was of an appropriate condition for the synthesis of purified diamond with good crystallinity. Its plasma species are considered to be composed of the following

(i) A large number of CH_3 radicals which are suitable for diamond synthesis.

(ii) A small number of C_2H_2 which accelerates polyacetylene deposition.

(iii) A large number of atomic hydrogen which suppresses polyacetylene formation by stabilizing dangling bonds of carbon atoms and polyacetylene chains on a growing surface.

C_2H_2 was suggested as a responsible precursor for polyacetylene component. This idea is consistent with the earlier studies of diamond growth in a C_2H_2–O_2 flame [21], in which the addition of oxygen was found to reduce C_2H_2 concentration in a flame, and diamond deposition was possible in the feed gas ratio (C_2H_2–O_2) of 0.7–1.0 [22] where C_2H_2 production in the gas phase was heavily suppressed by their mass spectroscopic results [21].

There is another report suggesting that C_2H_2 is responsible for polyene structure. An earlier report [23] investigated the exhaust gas of a CH_4–H_2 tungsten filament-assisted diamond deposition system using gas chromatography, and found that the addition of O_2 suppressed both C_2H_2 production in the gas phase and deposition of non-diamond phases.

5. Conclusions

A variety of diamond films were deposited using the microwave plasma of a CO–H_2 system. Qualities of synthesized films were correlated with the gas phase atomic hydrogen concentration monitored using optical emission spectroscopy. The amorphous components contained in synthesized films were identified as a polyacetylene structure, which was possibly formed by the successive polymerization of C_2H_2 in the gas phase.

An excess atomic hydrogen environment allowed highly crystallized diamond films containing only a small amount of polyacetylene components to be deposited at high growth rates. Two reasons were considered to explain these results. Under the excess atomic hydrogen condition, polyacetylene can be suppressed to deposit by filling dangling bonds of carbon atoms and polyacetylene chains on a growing surface with atomic hydrogen. This results in the selective growth of diamond polycrystallites.

In reference to a previous work [13], the mole fraction ratios of CH_3 to C_2H_2 ($C[CH_3]/C[C_2H_2]$) were considered to become larger on increasing atomic hydrogen concentration, thus, under the excess atomic hydrogen condition, a large amount of appropriate precursors (CH_3) for diamond synthesis and a small amount of polyacetylene precursors (C_2H_2) were thought to be produced, resulting in enhancement of the growth of highly purified diamond with good crystallinity.

Finally, I_H/I_{Ar} defined in this paper was suggested as a decisive parameter to determine the suitability of plasma conditions for the growth of pure diamond films with good crystallinity.

References

1. R. J. NEMANICH, J. T. GLASS, G. LUCOVSKY and R. E. SHRODER, *J. Vac. Sci. Technol.* **A6** (1988) 1783.
2. W. ZHU, C. A. RANDALL, A. R. BADZIAN and R. MESSIER, *ibid.* **A7** (1989) 2315.
3. Y. SAITO, K. SATO, H. TANAKA, K. FUJITA and S. MATSUDA, *J. Mater. Sci.* **23** (1988) 842.
4. J. A. MUCHA, D. L. FLAMM and D. E. IBBOTSON, *J. Appl. Phys.* **65** (1989) 3448.
5. Y. SAITO, K. SATO, K. GOMI and H. MIYADERA, *Proc. Jpn Symp. Plasma Chem.* **1** (1988) 303.
6. Y. MURANAKA, H. YAMASHITA, K. SATO and H. MIYADERA, *J. Appl. Phys.* **67** (1990) 6247.
7. J. W. COBURN and M. CHEN, *ibid.* **51** (1980) 3134.
8. K. KOBASHI, K. NISHIMURA, Y. KAWATE and T. HORIUCHI, *J. Vac. Sci. Technol.* **A6** (1988) 1816.
9. I. HARADA, *Chem. Lett.* (1978) 1411.
10. D. B. FITCHEN, *Mol. Crystallogr. Liq. Crystallogr.* **83** (1982) 95.
11. H. KUZMANY, E. A. IMHOFF, D. B. FITCHEN and A. SARHANGI, *Phys. Rev.* **B26** (1982) 7109.
12. E. MULAZZI and G. P. BRIVIO, *Solid State Commun.* **46** (1983) 851.
13. R. MACH, *Beitr. Plasmaphys.* **23** (1983) 595.
14. F. KAUFMAN, *Adv. Chem. Ser.* **80** (1969) 29.
15. J. J. LANDER and J. MORRISON, *Surf. Sci.* **4** (1966) 241.
16. F. G. CELLI and J. E. BUTLER, *Appl. Phys. Lett.* **54** (1989) 1031.
17. M. TSUDA, M. NAKAJIMA and S. OIKAWA, *J. Amer. Chem. Soc.* **108** (1986) 5780.
18. F. G. CELLI, P. E. PEHRSSON, H. T. WANG and J. E. BUTLER, *Appl. Phys. Lett.* **52** (1988) 2043.
19. M. KAMO, Y. SATO and N. SETAKA, *Nippon Kagaku Kaishi*, **10** (1984) 1642.
20. S. J. HARRIS and A. M. WEINER, *Appl. Phys. Lett.* **53** (1988) 1605.
21. Y. MATSUI, A. YUUKI, M. SAHARA and Y. HIROSE, *Jpn J. Appl. Phys.* **28** (1989) 1718.
22. Y. HIROSE, *Electronic Parts and Materials*, **28** (1989) 45.
23. T. KAWATO and K. KONDO, *Jpn J. Appl. Phys.* **26** (1987) 1429.

Received 30 April
and accepted 13 August 1990